



## IMAGE IN IMAGE STEGANOGRAPHY USING WAVELET TRANSFORM

Sonia A. R. Mohammed Ali  
Dept. of Electronic and Communication Engineering  
College of Engineering  
University of Baghdad

### ABSTRACT

This paper describes a stego system in which a gray scale image is embedded in another one. Wavelet transform of both the cover image and the embedded image is used to sort their subband's energies to guarantee that the embedded image will be inserted in the low frequency components of the cover image with little perceptual distortion.

Embedding by this way increases the robustness of the system but affects the system's imperceptibility, so a variable scaling factor ( $\alpha$ ) is used to attenuate the components of the embedded image before adding them to those of the cover image.

It is found that the stego image with peak signal-to-noise ratio (PSNR) of about 30 dB has good imperceptibility.

The attacker is proposed to be active, so compression is applied to the stego image. According to this, the scaling factor must be increased to compromise between the quality of the stego and the reconstructed images. This increment reduces the imperceptibility of the stego image and here the trade off between the imperceptibility and the robustness occurs.

The attack is proposed to be stego known, so that to increase the security of the system, a stego key is generated from the embedded image itself and is transmitted separately, making the system type secret key steganography.

The size of the embedded image obtained in the work is one quarter the size of the cover image that may be considered good comparing with the available systems.

### الخلاصة

في هذا البحث يتم وصف نظام إخفاء صوري و الذي يتم من خلاله إخفاء صورة رمادية المقياس في صورة أخرى رمادية المقياس أيضا.

استخدم تحويل الموجة لكل من الصورة الغطاء و الصورة المضمورة لكي يتم تصنيف حزم الطاقة الفرعية للتأكد من وضع الصورة المضمورة في مركبة الترددات الواطنة للصورة الغطاء مع تشويهِ غير محسوس.

هذه الطريقة تزيد من متانة النظام ولكنها تؤثر على اللاقابلية لإدراك الصورة، لهذا السبب استخدم عامل تبديل لتضعيف قيمة مركبات الصورة المضمورة قبل إضافتها الى مركبات الصورة الغطاء.

لذد وجد إن الصورة الناتجة من الإخفاء تكون ذات نوعية جيدة عندما تكون نسبة الذروة للإشارة مقابل الضوضاء (نذ/ض) أعلى من 30 ديسيبل.

اقترح أن يكون المهاجم فعالا لذا تم تطبيق كبس الصورة الناتجة لبيان تأثير الهجوم مما أدى وجوب زيادة عامل التعبير للموازنة بين الصورة الناتجة والصورة المعاد تشكيلها، وهذه الزيادة الطفيفة تقلل نسبيا اللاقابلية على إدراك الصورة الناتجة وهنا تحدث المقايضة بين هذه اللاقابلية على الإدراك وبين المتانة. اقترح أن تكون الهجمة مشخصة من قبل المهاجم، لذا لزيادة أمنية النظام، يولد مفتاح الإخفاء من الصورة المطمورة نفسها وبهذا يكون النظام من نوع إخفاء بالمفتاح السري. حجم الصورة المطمورة في هذا العمل هو ربع حجم الصورة الغطاء وهكذا يمكن أن يعد هذا النظام ذو استيعابية جيدة.

## KEY WORDS

Steganography; information hiding; image hiding.

## INTRODUCTION

Moves to restrict the availability of services have motivated people to study methods by which private messages can be embedded in seemingly innocuous cover messages (Stefan and Fabien 2000).

One of the newest methods in security researches is information hiding. An important subdiscipline of information hiding is steganography. While cryptography is about protecting the content of messages, steganography is about concealing their very existence (Stefan and Fabien 2000). Steganography literally means "covered writing" and is the art of hiding the very existence of a message. The possible cover carriers are innocent looking carries (images, audio, video, text or other digitally representative code) which will hold the hidden information. A message is the information hidden and may be plaintext, ciphertext, images or anything that can be embedded into a bit stream. Together the cover carrier and the embedded message create a stego carrier (Jack and Larry 1996), (Areepongsa et al 2000).

Hiding information may require a stegokey, which is additional secret information (Christian 1998). For example, when a secret image is hidden within a cover image, the resulting product is a stego image. A possible formula of the process may be presented as (Neil et al 2001):

Cover medium + embedded message + stegokey = stego medium

Many steganographic methods have been proposed during the past few years. Most try to substitute redundant part of the signal with a secret message; their main disadvantage is the relative weakness against cover modification.

It has been noted early in the development of steganographic systems that embedding information in the frequency domain of a signal can be much more robust than embedding rules operating in the time domain. Most robust steganographic systems known today actually operate in the same sort of transform domain (Stefan and Fabien 2000).

Transform domain methods hide messages in the significant areas of the cover image, which makes them more robust to attacks such as adding noise, compression, filtering and some image processing. However, while they are more robust to various kinds of signal processing, they remain imperceptible which means that the human visual system (HVS) has no sense that there exists a stego-image (Ingemar et al 1996).

In this paper the discrete time wavelet transform (DTWT) is used as the transform technique in the steganography process to increase its robustness by inserting the embedded image in the low frequency component of the cover image in order to reduce the effect of the attacker. The system is subjected to a compression attack to see how it will affect the reconstructed image.

## IMAGE EMBEDDING

It is well known that embedding in the low frequency bands is more robust to manipulations. However, changes made to the low frequency component may result in visible artifacts (Abdulaziz and Pang 2000). Modifying the data in a multiresolution framework, such as a wavelet transform appears quite promising for obtaining quality embedding with little perceptual distortion. Fig. 1 shows the whole embedding process, which will be explained in the following section.

### Partition the Cover and the Embedded Images into Subbands

The whole process can be described as follows, denoting the original image by  $I_0$ , assuming its size is  $2^l \times 2^l$ . After applying the two-dimensional discrete time wavelet transform (2-D DTWT) to it, one can get a matrix  $I_1$  partitioned into four subbands. The 2-D DTWT is applied to each of these bands individually. The result is the coefficient matrix  $I_1$  consisting of 16 subbands, when this process is carried out  $r$  times, a coefficient matrix consisting of  $2^r \times 2^r$  subbands, each of size  $2^{l-r} \times 2^{l-r}$  (Salomon 2000) is obtained.

The main job of applying the wavelet packets to both the cover image and the embedded image in the proposed stegosystem is to partition these images into subbands in which each subband has certain frequency information. Since most of the natural images' energy concentrates in the low frequency band, then in general, the high energy subbands reflect their low frequency contents and vice versa.

The size of the embedded image is chosen to be quarter the size of the cover image to ensure that the entire embedded image be completely inserted in the LL subband of the cover image.

The number of the decomposition levels that are applied to the embedded image is less by one than those applied to the cover image so that the number of coefficients in each subband in both transformed images are equal.

### Generation of The Stego-key by Sorting Process

After applying the full tree two-dimensional wavelet packets to both the cover and the embedded images, subbands that contain both the frequency and spatial information are obtained. The energy ( $E_i$ ) of each subband is then calculated as follows

$$E_i = \sum_{j=1}^{\frac{N}{2^i}} \sum_{k=1}^{\frac{N}{2^i}} S_i^2(j, k) \quad i = 1, 2, \dots, 4^l$$

Where  $l$  is the decomposition level.

$N \times N$  dimension of the input image

$S_i$  order of each subband

The subbands of both the cover and the embedded images are then sorted in a descending manner such that the highest energy is the first and the least energy subband is the last. **Table (1)** illustrates the energies of all subbands resulting from the sorting process of two levels of decomposition applied to 256 x 256 gray level version of Lena standard image.

This sorting process will increase the robustness of the system and improve the security of the proposed stego-system by considering the order of the embedded image subbands as a stego-key.

Table (1) Illustrating the sorting and the scaling processes

Subbands	S <sub>i</sub>	Corresponding Energies	Sorted Subbands	Sorted S <sub>i</sub>	Corresponding Energies	Scaling Factor α <sub>i</sub>
LLLL	S <sub>1</sub>	801838270	LLLL	S <sub>1</sub>	801838270	0.5
LLLH	S <sub>2</sub>	2204826	LLHL	S <sub>3</sub>	6751748	0.531
LLHL	S <sub>3</sub>	6751748	LLLH	S <sub>2</sub>	2204826	0.562
LLHH	S <sub>4</sub>	1360912	HLHL	S <sub>11</sub>	1815081	0.593
LHLL	S <sub>5</sub>	199427	LLHH	S <sub>4</sub>	1360912	0.625
LHLH	S <sub>6</sub>	478589	HLLL	S <sub>9</sub>	664613	0.656
LHHL	S <sub>7</sub>	143275	HLHH	S <sub>12</sub>	608941	0.687
LHHH	S <sub>8</sub>	418153	LHLH	S <sub>6</sub>	478589	0.718
HLLL	S <sub>9</sub>	664613	LHHH	S <sub>8</sub>	418153	0.750
HLLH	S <sub>10</sub>	243747	HHHH	S <sub>16</sub>	301075	0.781
HLHL	S <sub>11</sub>	1815081	HLLH	S <sub>10</sub>	243747	0.812
HLHH	S <sub>12</sub>	608941	LHLL	S <sub>5</sub>	199427	0.843
HHLL	S <sub>13</sub>	80472	HHLH	S <sub>14</sub>	148554	0.875
HHLH	S <sub>14</sub>	148554	LHHL	S <sub>7</sub>	143275	0.906
HHHL	S <sub>15</sub>	107074	HHHL	S <sub>15</sub>	107074	0.937
HHHH	S <sub>16</sub>	301075	HHLL	S <sub>13</sub>	80472	0.968

### The Scaling Process

In the proposed stego system the embedded image is inserted in the low frequency region of the cover image which is a perceptually significant region to confirm the robustness of the system. This will affect the imperceptibility of the system. To compromise between the two parameters, a variable factor  $\alpha$  is chosen which is multiplied by the coefficients of the cover image to attenuate their values. The scaling factor is dependent on the subband energy. In other words, the coefficients of the high-energy subbands are multiplied by factors, which are less than the corresponding factors of the low energy subbands. The scaling factors are calculated by the following equation

$$\alpha_i = \alpha_{\min} + \left\{ (i-1) \times \frac{\alpha_{\min}}{4^{\ell}} \right\} \quad i = 1, 2, 3, \dots, 4^{\ell}$$

Where  $\alpha_{\min}$  is the scaling factor that attenuates the highest energy subbands.

**Table (1)** gives the scaling factors for two levels decomposition of Lena Image that is shown in **Fig.(2)** with  $\alpha_{\min}$  chosen to be 0.5.

After this scaling process, one can easily insert the low frequency regions of the embedded image to the low frequency of the cover image to produce a robust stego image. The value of  $\alpha_{\min}$  must be sent via a secret channel with the stego key to the receiver.

### The Re-sorting Process

The resultant stego image is not identical to the cover image due to the sorting process, because the resultant subbands are not arranged in the same order of the cover image subbands. But, from the steganography viewpoint the two images must be identical. For this reason, the need for a re-sorting process arises. In this process the subband, that consists of the cover image subbands added to the attenuated version of the embedded subbands are resorted in the same order of the cover image subbands, such that the stego image will be approximately identical to the cover image.

### The Inverse Wavelet Packet Transform

After the resorting process, the sequences of the cover image subbands and the stego image are identical but their frequency contents are not due to the addition of the attenuated embedded image subbands.

Applying the inverse wavelet packet transform to the stego-image subbands followed by a quantization process will produce a stego image with little degradation.

The wavelet filters and the number of the decomposition levels must be the same in the wavelet packets and the inverse wavelet packets. The pixels of the stego image after the inverse transform are not quantized as a gray scale. So that a uniform quantization is applied to this image to preserve the initial dynamic range of the cover image. For 256 subdivisions, uniform quantization can be done as follows

$$f_q(r,c) = \left\{ f(r,c) - f_{\min} \right\} \frac{255}{(f_{\max} - f_{\min})}$$

Where  $f(r,c)$  is the image before quantization and  $f_q(r,c)$  is the quantized version of it,  $f_{\max}$  and  $f_{\min}$  are the maximum and the minimum values in the original image respectively

**Fig. (2)** shows the images after each block of **Fig.(1)** for the embedding process. In order to visually recognize the differences between these images, the decomposition levels of the cover and the embedded images are chosen to be two and one respectively (for an example only).

The flow chart of the embedding process is shown in **Fig.(3)**.

### **IMAGE EXTRACTING**

If the original cover image with the stego-image, the stego key and  $\alpha_{\min}$  are available to the receiver, then the extraction of the embedded image is possible.

The stego-image is transmitted via a public communication channel, while the stego-key and  $\alpha_{\min}$  are transmitted via a secret channel.

Applying the wavelet packet transform first produces the subbands of the cover image and the stego image. The subbands of the stego image contain the cover image subbands added to those of the embedded image. Then a descending sorting process is applied to the produced subbands. The cover image subbands are then subtracted from the stego image subbands, coefficient by coefficient and the resulted coefficients are multiplied by the reciprocal of the scaling factor to amplify them to their original values to get the coefficients of the embedded image. The stego key that contains the original sequence of the embedded image subbands is used to resort the resultant subbands such that the embedded image can be reconstructed by applying the inverse wavelet packets followed by the quantization process.

The filters and the number of the decomposition levels that are applied to both the stego and the cover images must be identical to those used in the embedding process.

**Fig. (4)** shows the images after each block of **Fig. (1)** for the extracting process. The flow chart of the extracting process is shown in **Fig. (5)**.

## THE ROBUSTNESS OF THE SYSTEM

Since in the proposed stego system the frequency domain has been selected to embed the entire image, it is required to be a robust system. The robustness of the proposed system will be tested against compression attack

### The Compression Test

The JPEG (Salomon 2000) compression is used here because it is a standard lossy compression algorithm that uses many parameters allowing users to adjust the amount of the data lost (and thus also the compression ratios) over a wide range.

The compression ratios that are used in this work is 5, 7.5 and 10. These ratios can be obtained by adjusting the factor that multiplies the quantization matrix.

The coding part of the JPEG algorithm is not implemented in this work because it is the lossless part, therefore it is not useful to be used.

The results of this test will be discussed in the following section.

## EXPERIMENTAL RESULTS

The test images used in this work are shown in **Fig.(6)** in Image 1 and Image 5. The cover image is the Lena Image with 256 x 256 pixels and the embedded image is the Saturn Image with 128 x 128 pixels as shown in Image 1 and Image 5 respectively.

The proposed stego system uses different decomposition levels and the variable scaling factor  $\alpha$  and then selects optimum parameters to compromise between the quality of both the stego and the reconstructed images.

A Daubechies (Burrus et al 1998) filter with four-coefficient ( $D_4$ ) is used in the wavelet packets and its inverse in both the embedding and the extracting process as a wavelet filter.

**Table (2)** shows the PSNR's for both the stego and the reconstructed images for three different decomposition levels and with variable scaling factor  $\alpha$ . For four decomposition levels applied to the cover image, and three decomposition levels applied to the embedded image, one can notice that the PSNR's of the stego-image increases with decreasing  $\alpha_{\min}$  which means that the scaling factor does its job properly. The results of the other decomposition levels (five and six) are in the same context but with noticeable improvement. When the number of the decomposition levels increases, the energies of the embedded image's subbands will be distributed equally and there are no subbands in which the energy is concentrated.

Table (2) PSNRs (dB) for the reconstructed images

$\alpha_{\min}$ \ DL	Four Levels		Five Levels		Six Levels	
	Stego	Recon.	Stego	Recon.	Stego	Recon.
0.5	21.13	37.33	21.13	40.71	21.15	43.51
0.4	23.05	35.78	23.06	39.38	23.07	44.12
0.3	25.52	33.44	25.55	36.93	25.57	41.98
0.2	28.99	30.14	29.05	33.42	29.08	38.62
0.1	34.69	24.56	34.95	27.49	35.07	32.82
Optimum Parameters	$\alpha_{\text{opt.}}=0.18$ PSNR=29.5 dB		$\alpha_{\text{opt.}}=0.155$ PSNR=31.25 dB		$\alpha_{\text{opt.}}=0.12$ PSNR=34 dB	

As a result the effect of the quantization process will be decreased and improvement in the result occurs. In this case increasing of the decomposition levels increases the security of the system that is not conflicted with the imperceptibility of the stego system, so that one can select both requirements and there is no need for trade off between them. The optimum scaling factor  $\alpha_{\text{opt}}$  is the

value of  $\alpha$  where the PSNR's of the stego and reconstructed images are equal which is shown in Fig. (7) for different decomposition levels. The last row of Table (2) lists  $\alpha_{opt}$  and the corresponding PSNR's. The corresponding images for these results are shown in Fig. (6) in the Images 2, 3, 4, 6, 7 and 8.

The size of the embedded image which is used in this system is one quarter the size of the cover image and this capacity is considered as being good when comparing with the most of the existence systems (Marza 2001),(Avedissian 2000),(Ibrahim 2001).

If the size of the embedded image is increased, part of this image will be inserted in the high frequency of the cover image that may be affected by compression. Obviously, if the size of the image is decreased there is an improvement in the imperceptibility of the stego-image.

The proposed system is assumed to be a secret key stego system. The stego-key is generated from the embedded image itself by considering its sorted subband's sequence as a stego-key. The sequence differs from one image to another because there are no two identical images in nature. The subband's order for different images are changed in different ways, except the first subband that represents the low frequency in both direction and it is expected that its order will not be changed because it still has the largest energy, so that the number of the possible keys that can be generated is  $(4^l - 1)!$ .

Table (3) shows the results of the compression tests at different decomposition levels,  $\alpha$  and compression ratios. These results are plotted in Fig.(7). Comparing with the results obtained without compression (i.e with CR=1), generally, the PSNR's of the reconstructed images decrease due to compression. This reduction in PSNR grows as the compression ratio increases but the results are still acceptable. To compromise between the stego and the reconstructed images,  $\alpha_{opt}$  must be relatively increased to reduce the imperceptibility of the stego image as a price to this resistant against the compression attack.

Finally, Table (4) shows the optimum parameters with the corresponding compromised PSNR of the stego and the reconstructed images under test. It is clear that  $\alpha_{opt}$  is increased for about 0.05 to 0.12 causing a decrease in the PSNR's for about 1.5 to 6 dB. For six decomposition levels the corresponding images of Table (4) are shown in Fig.(8) in Images 9, 10, 11, 12, 13, and 14.

Table (3) PSNRs (dB) for the reconstructed images for JPEG compression tests

$\alpha_{min}$ \ CR	Four Levels			Five Levels			Six Levels		
	5	7.5	10	5	7.5	10	5	7.5	10
0.5	32.99	28.88	25.98	33.55	28.84	26.1	33.96	29.09	26.3
0.4	31.35	27.23	24.43	32.15	27.35	24.53	32.25	27.58	24.51
0.3	29.21	25.23	22.4	29.82	25.19	22.39	30.05	25.33	22.41
0.2	26.05	22.08	18.91	26.76	22.45	19.11	27.06	22.5	19.2
0.1	20.76	16.52	13.83	21.4	16.58	13.92	21.04	16.76	13.97

Table (4) The optimum parameters for JPEG compression tests

CR	FOUR LEVELS		FIVE LEVELS		SIX LEVELS	
	$\alpha_{opt}$	PSNP	$\alpha_{opt}$	PSNP	$\alpha_{opt}$	PSNP
5	0.235	28	0.2240	27.9	0.225	28
7.5	0.308	25.5	0.3025	25.7	0.3	26.2
10	0.362	24	0.3610	24.2	0.36	24.25

## CONCLUSIONS

Through the simulation results, one can conclude that:

- The quality of both stego and reconstructed images is considered good with PSNR is above 30 dB.
- Increasing the number of the decomposition levels which increases the security of the system is not conflict with the imperceptibility of the stego image. The PSNR is increased by about 4.5 dB if the decomposition levels are six rather than four.
- As the JPEG compression ratio increased,  $\alpha$  must be increased and hence the PSNR of the stego and the reconstructed images is reduced.
- The size of the embedded image is one quarter the size of the cover image, which is considered relatively good when compared with the present stego systems.
- There is still some work to be done. The stego system needs to be subjected to attacks, such as noise addition, filtering, and other processing techniques and see how it will affect the reconstructed image.

## REFERENCES

Christian Cachin (1998), "An Information-Theoretic Model for Steganography", Information Hiding; Second Int. Workshop Proc., Portland, Oregon, USA.

D. Salomon (2000) "Data Compression, the Complete Reference", Springer-Verlag. New York, In.

H. H. Marza (2001), "Text in Image Steganography Techniques", M.Sc. Thesis, Computer Science Dept., College of Science, University of Baghdad, Baghdad, Iraq.

Ingenar J. Cox, Joe Kilian, Tom Leighton and Talal Shamoan (1996), "A Secure, Robust Watermark for Multimedia", Information Hiding; First Int. Workshop Proc., Cambridge, U.K., May 30- June 1.

Jack Brassl and Larry O'Gorman (1996), "Watermarking Document Images with Bounding Box Expansion", Information Hiding; First Int. Workshop Proc., Cambridge, U.K., May 30- June 1.

L.Z. Avedissian (2000), "Image in Image Steganography", Ph. D. Thesis, Computer Science Dept., College of Science, University of Technology, Baghdad, Iraq.

Neil F. Johnson, Zoran Duric, and Sushil Jajodia (2001), " INFORMATION HIDING: Steganography and Watermarking-Attacks and Countermeasure", Kluwer Academic Publishers .

N. K. Abdulaziz and K. K. Pang (2000), "Robust Data Hiding for Images", Proc. IEEE, pp. 380 - 383.

S. Areepongsa, Y. F. Syed, N. Naewkamnerd, and K. R. Rao, "Steganography for a Low Bit- Rate Wavelet Based Image ", <http://issu.gmu.edu/~njohnson/steganography>.

S. Burrus, R. Gopinath, and H. Guo (1998), " Introduction to Wavelets and Wavelet Transform", Upper Saddle, New Jersey: Prentice Hall.

Stefan Katzenbeisser and Fabien A. P. Petitcolas (2000), "Information Hiding Techniques for Steganography and digital Watermarking", Artech House.

U. I. Ibrahim (2001), "Text in Image Steganography", M. Sc., Computer Science Dept., College of Science, University of Technology, Baghdad.

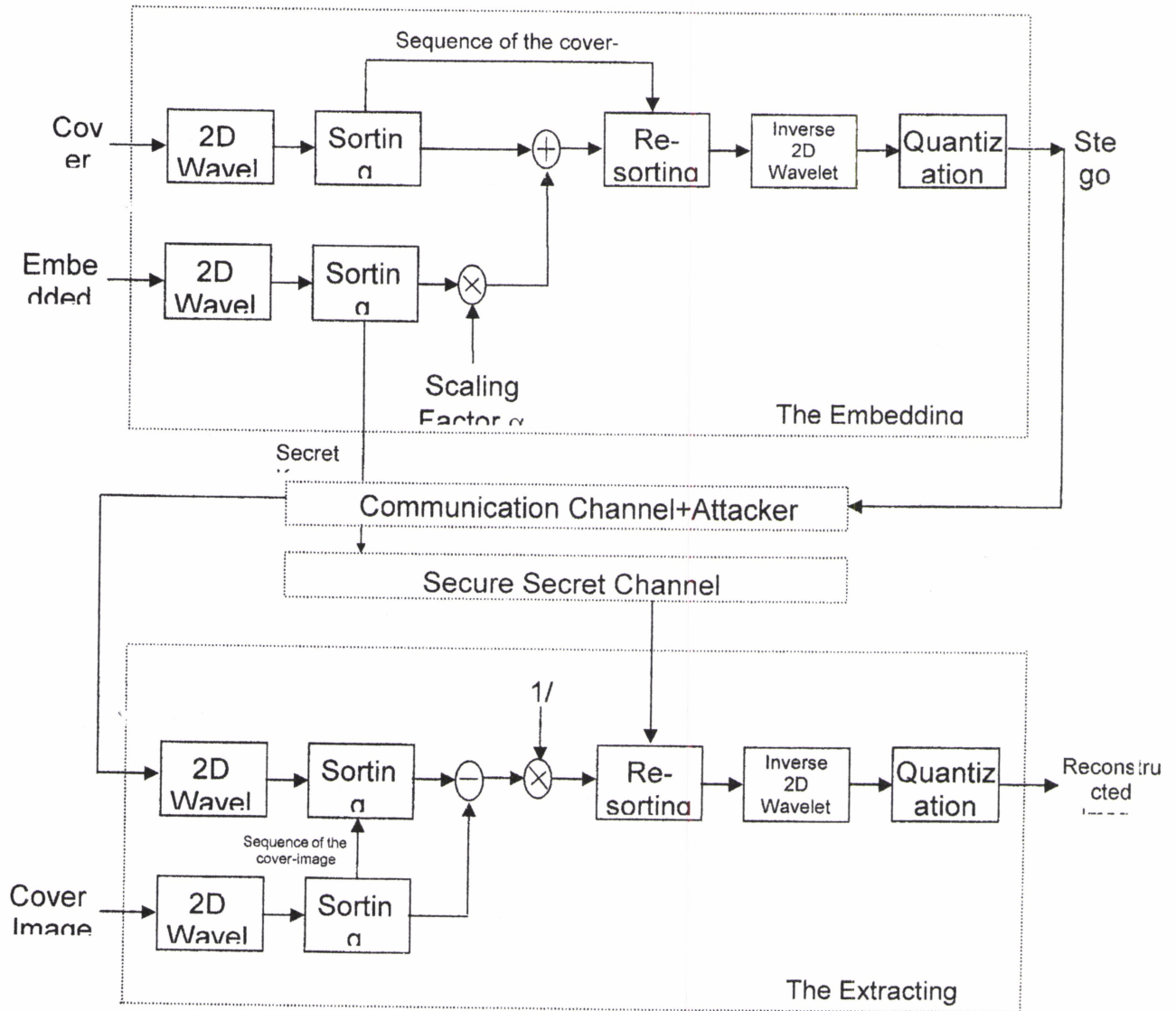


Fig. (1) The Proposed Stego-

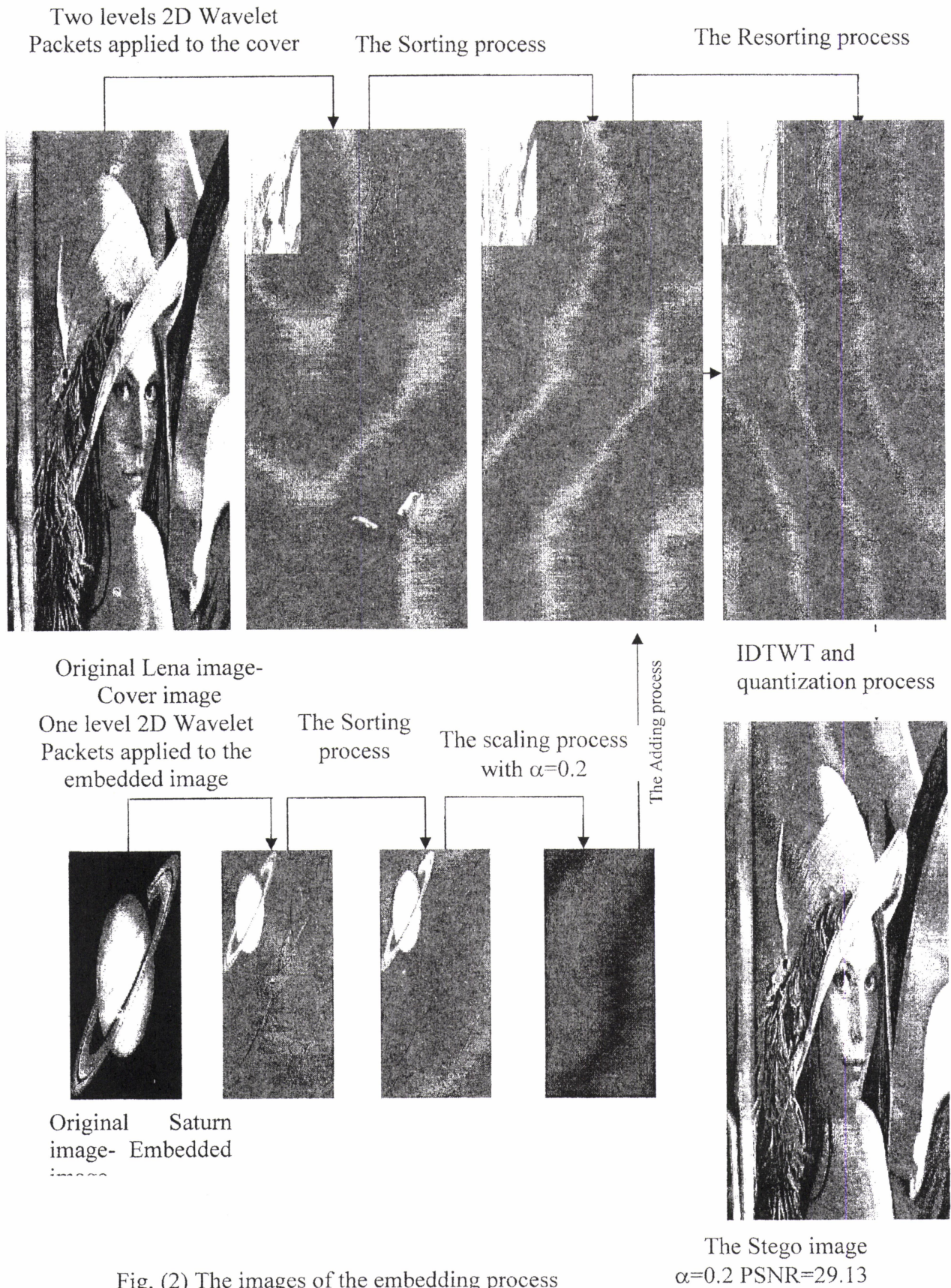


Fig. (2) The images of the embedding process

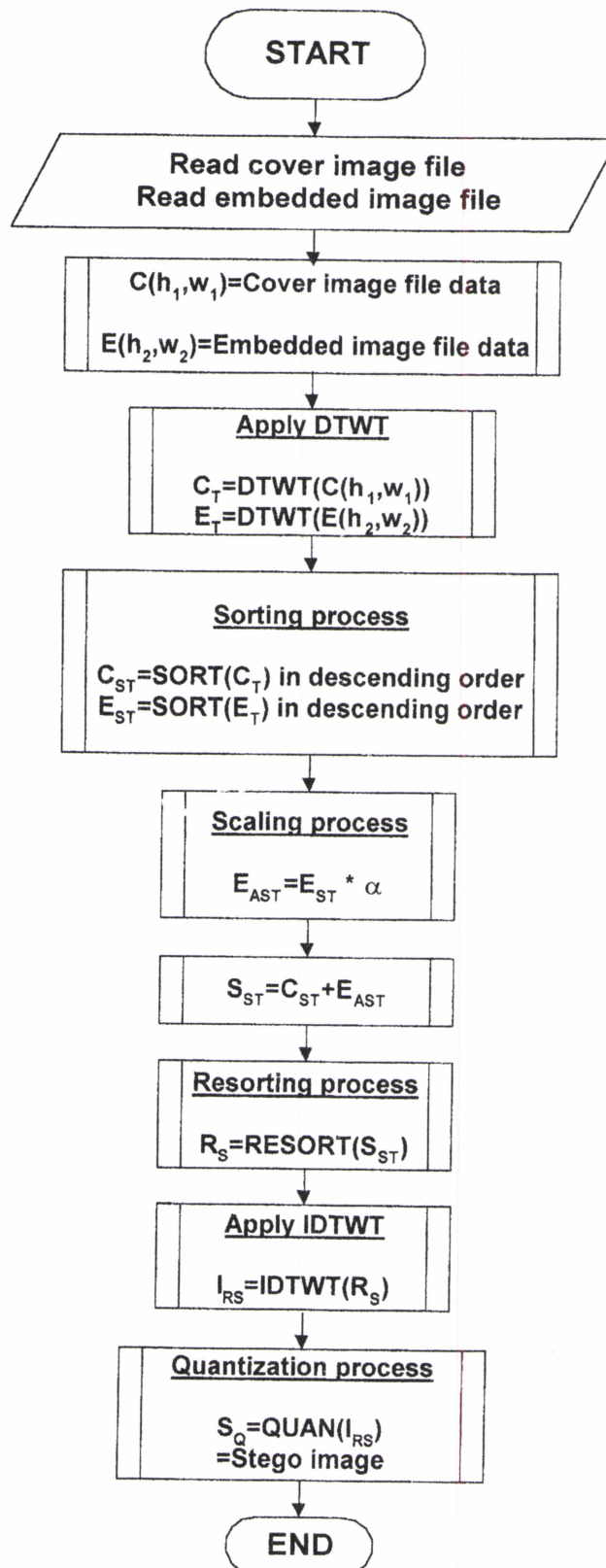


Fig. 3 The flow chart of the embedding process

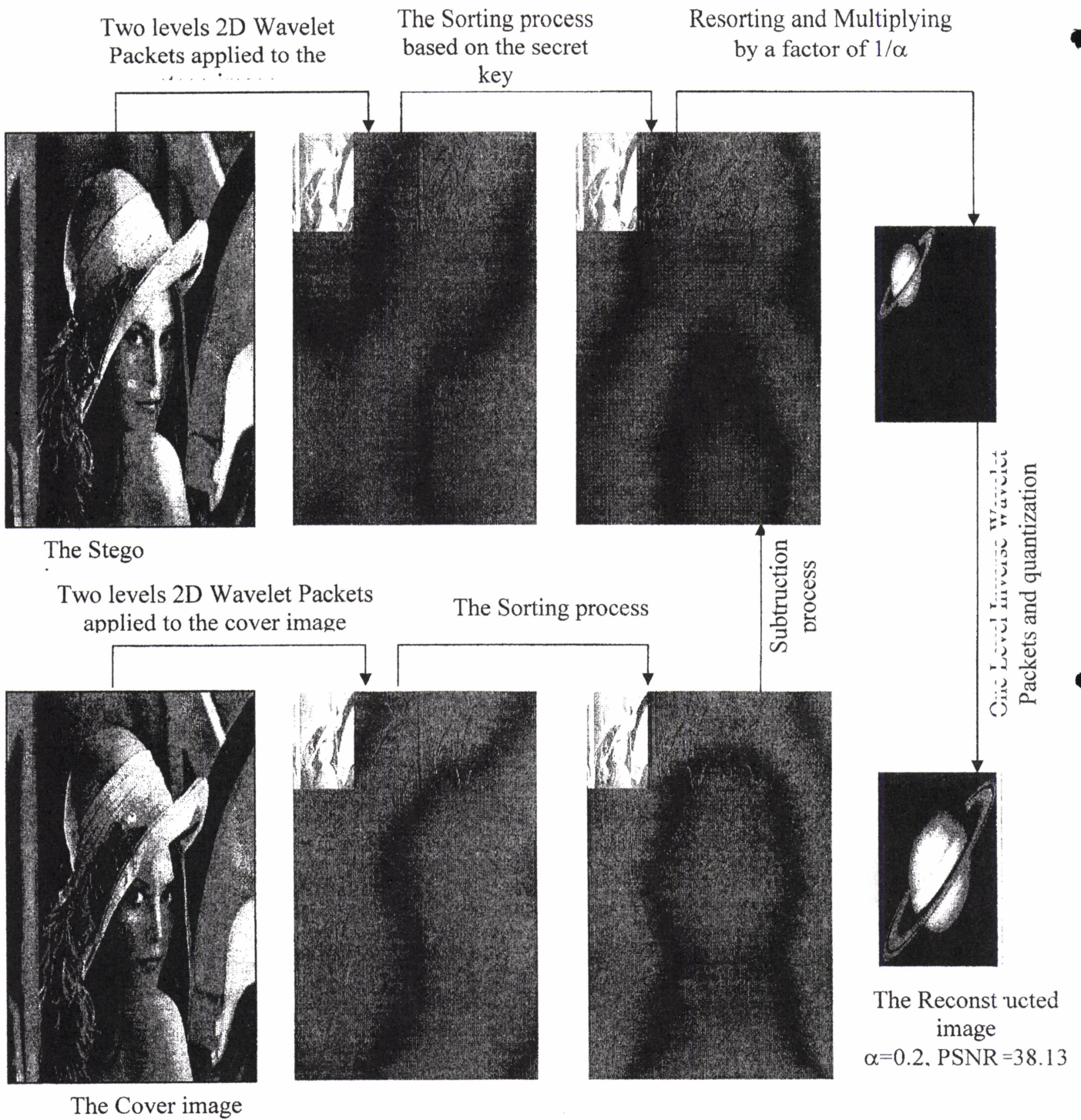


Fig.(4) The images of the extracting process

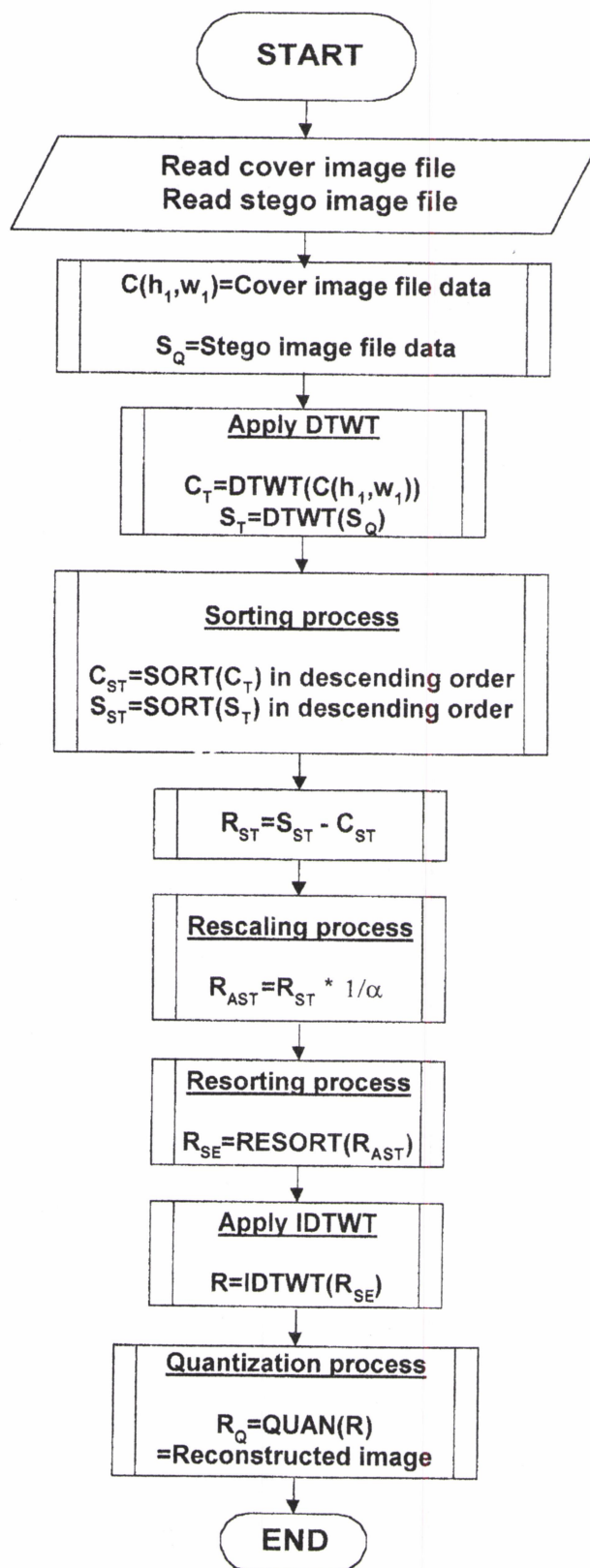


Fig. (5) The flow chart of the extracting process



Image 1 Original Lena image



Image 2 Stego image  
Four decomposition levels  
 $\alpha_{opt}=0.18$  PSNR=29.5



Image 3 Stego image  
Five decomposition levels  
 $\alpha_{opt}=0.155$ , PSNR=31.5



Image 4 Stego image  
Six decomposition levels  
 $\alpha_{opt}=0.12$ , PSNR=34 dB

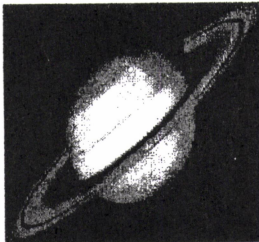


Image 5  
Original Saturn  
image

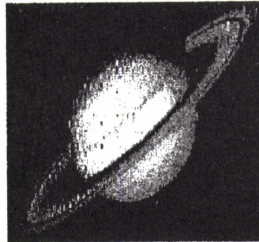


Image 6  
Reconstructed  
image related  
to image 2

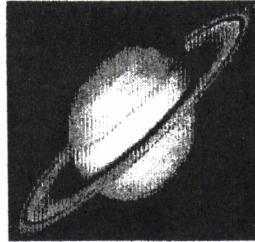


Image 7  
Reconstructed  
image related  
to image 3

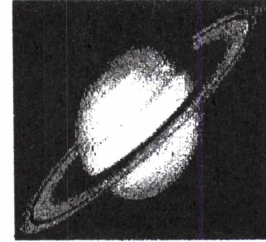
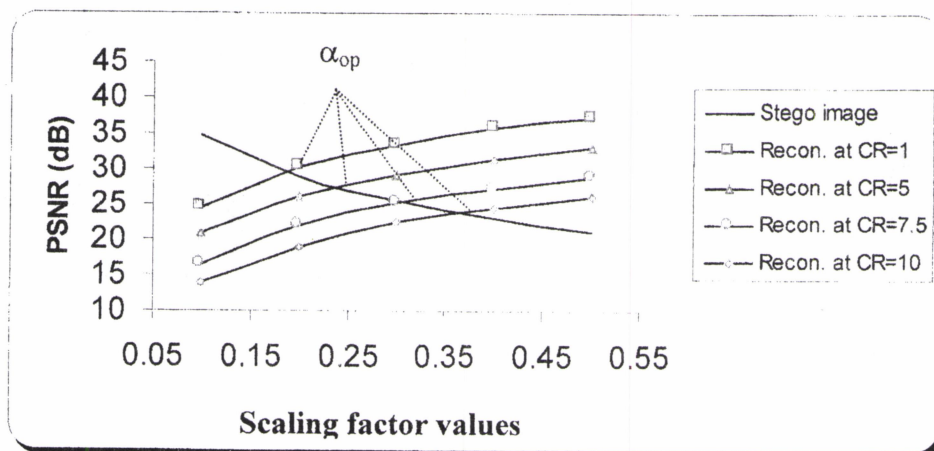
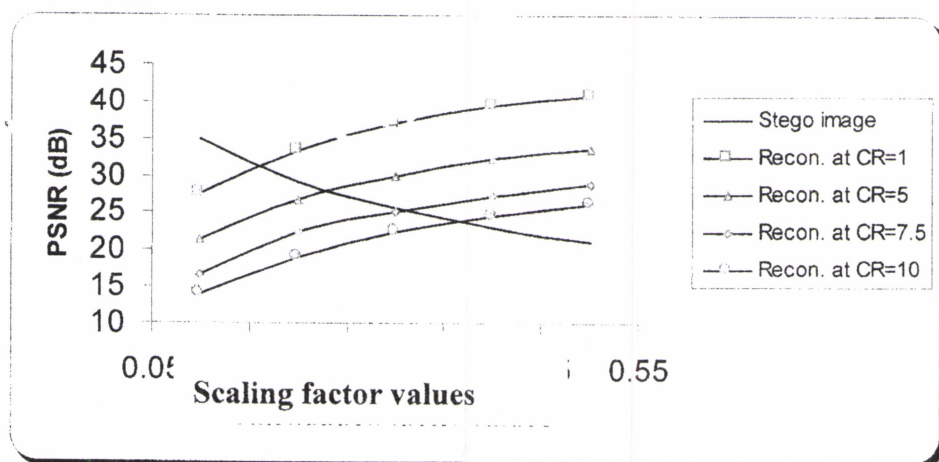


Image 8  
Reconstructed  
image related  
to image 4

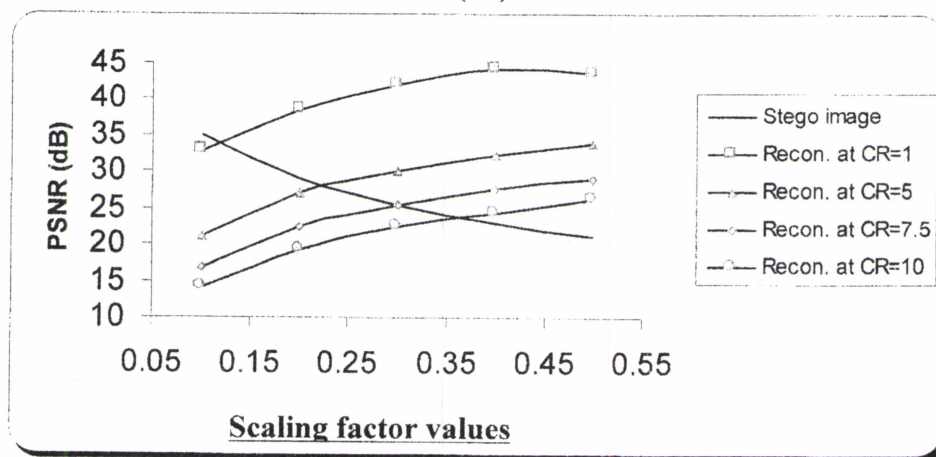
Fig. (6) The stego images and the corresponding reconstructed images for different parameters



(a)



(b)



(c)

Fig.(7) PSNR's for both stego and reconstructed images vs. the scaling factor for:  
(a) Four decomposition levels and different compression ratios  
(b) Five decomposition levels and different compression ratios  
(c) Six decomposition levels and different compression ratios



**Image 9 Stego image**  
Six decomposition levels  
 $\alpha_{opt}=0.225$ , PSNR=28 dB  
Compression ratio=5



**Image 10 Stego image**  
Six decomposition levels  
 $\alpha_{opt}=0.3$ , PSNR=26.2 dB  
Compression ratio=7.5



**Image 11 Stego image**  
Six decomposition levels  
 $\alpha_{opt}=0.36$ , PSNR=24.25

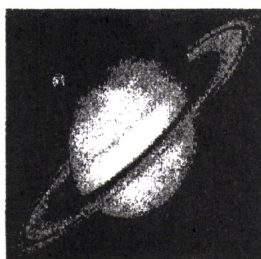


**Image 12**  
Reconstructed image  
related to image 9

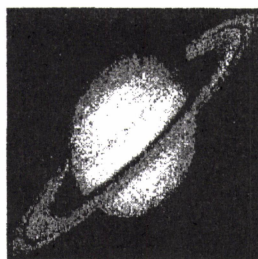


**Image 13**  
Reconstructed image  
related to image 10

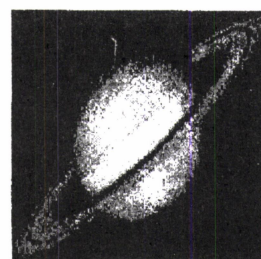


**Image 14**  
Reconstructed image  
related to image 11

Fig. (8) The stego images and the corresponding reconstructed images of the compression test for different parameters